VOL. 9, NO. 9, SEPTEMBER 2014 ISSN 1819-6608
ARPN Journal of Engineering and Applied Sciences


www.arpnjournals.com

FEM ANALYSIS FOR CRITICAL COMPONENTS IN ENGINES SYSTEMS

Eugenio Pezzuti[1] and Giampiero Donnici[2]
[1]Faculty of Engineering, University of Rome Tor Vergata, via del Politecnico, Rome, Italy
[2]DIN - Department of Industrial Engineering, Alma Mater Studiorum University of Bologna, viale Risorgimento, Bologna, Italy
E-Mail: pezzuti@mec.uniroma2.it

ABSTRACT

This paper introduces a method to simplify a nonlinear problem in order to use linear finite element analysis. This approach improves calculation time by two orders of magnitude. It is then possible to optimize the geometry of the components even without supercomputers. In this paper the method is applied to a very critical component: the aluminium alloy piston of a modern common rail diesel engine. The method consists in the subdivision of the component, in this case the piston, in several volumes, that have approximately a constant temperature. These volumes are then assembled through congruence constraints. To each volume a proper material is then assigned. It is assumed that material behaviour depends on average temperature, load magnitude and load gradient. This assumption is valid since temperatures varies slowly when compared to pressure (load). In fact pressures propagate with the speed of sound. The method is validated by direct comparison with nonlinear simulation of the same component, the piston, taken as an example. In general, experimental tests have confirmed the cost-effectiveness of this approach [1-4].

Keywords: optimization, simulation, CAD, geometry, FEA.

1. INTRODUCTION

Nonlinear simulation of piston engines is not so simple as it may be expected. Even with most sophisticated FEA software, it is not rare that true performance is grossly underestimated. For example in an "old" 8 valves common rail piston engine, the limit was fixed by the manufacturer to be around 140 bar. During tests no problem arose up to 160 bar and in many cases 180 bar were reached without problems. Also temperature seems to be out of range, with critical values easily overcome. This fact is due to the fact that the peak pressure and temperatures are reached in very short time and the duration is also very short. The velocity factor could not be ignored in piston FEA.

Even with the proper data, simulation takes a long time. Very nonlinear analysis should be performed with complicated material Tables that should take into account temperature, velocity, stress and strain.

Convergence is then more difficult than usual and in many cases progressive analysis is required with step introduced manually into the CAD/FEA model. This process is very time-consuming and leads to errors.

Geometry optimization is beyond possibility and standard geometries are adapted to the many geometrical constraint already present. At first glance it is possible to identify the different "schools" followed by the different manufacturers. Very different geometries are adopted to solve the same problem. This fact may mean that the optimization level is not very high. For this reason a new approach is introduced in this paper. At first a FEA pure thermo dynamical analysis is carried out to individuate maximum temperature values and distribution. Then this continuous temperature 3D map is sampled into a discrete number of values, typically with 5 levels at most. This process permits to isolate volumes with the same temperature level. Then these volumes of the piston with equal temperature level are isolated as single 3D parts. Then the piston is reassembled to the original shape by using these 3D parts. The FEA analysis is performed by assuming that these parts have perfect adherence (continuity of displacements on the common surface boundaries). By giving the proper tangential elastic modulus to each part it is possible to perform linear analysis instead of highly nonlinear. This is due to the fact that large displacements cannot be present in piston, in order to preserve the functionality of the piston. The tangential elastic modulus depends on the temperature (obtained by the FEA thermo dynamical simulation) and on the pressure and pressure gradient (usually obtained by a 1D Gas dynamics simulation model of the engine). The linear simulation of this piston assembly with linear material models usually takes seconds on a Personal Computer. The highly nonlinear traditional method takes hours or days on a supercomputer with the strong possibility that convergence does not take place.
In the following example:

1.1. Material properties of the critical component

A good knowledge of the material properties is fundamental for any simulation. In this case the piston is made of the well known aluminium alloy 390-T5. This alloy is commonly used in high performance turbocharged diesel engines. The 390-T5 chemical and mechanical properties are summarized in Tables 1, 2 and Figures 1, 2:

Table-1. A390 data.

Chemical composition	
Component	**Weight. %**
Al	78
Cu	4 – 5
Fe	Max 1.3
Mg	0.45 – 0.65
Mn	16 – 18
Ti	Max 0.2
Zn	Max 0.1

Table-2. A390 properties.

Mechanical and physical properties		
Hardness	125	HB
Ultimate tensile stress	295	MPa
Yeld tensile stress	260	MPa
Young Modulus	81.35	°C
Melting temperature	648.88	°C
Specific thermal capacity	0.962	kJ/kg°C
Density	0.0157	kg/m^3

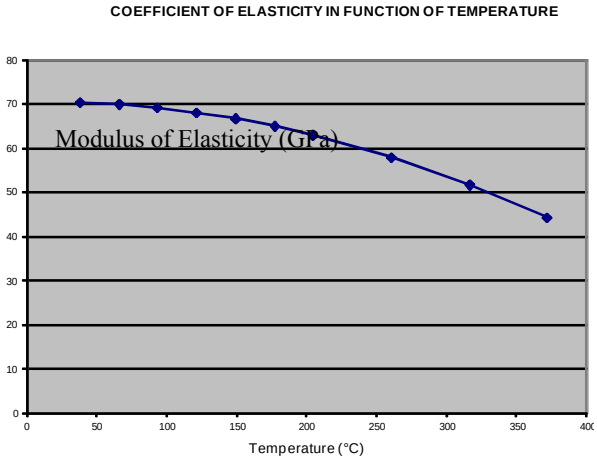

Figure-1. The static modulus of elasticity in function of temperature.

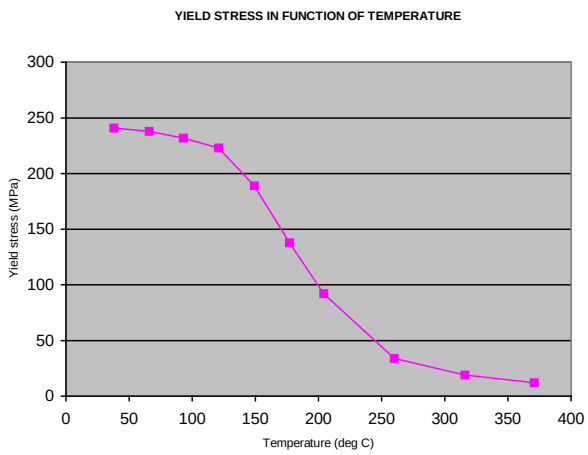

Figure-2. The static yield stress in function of the temperature.

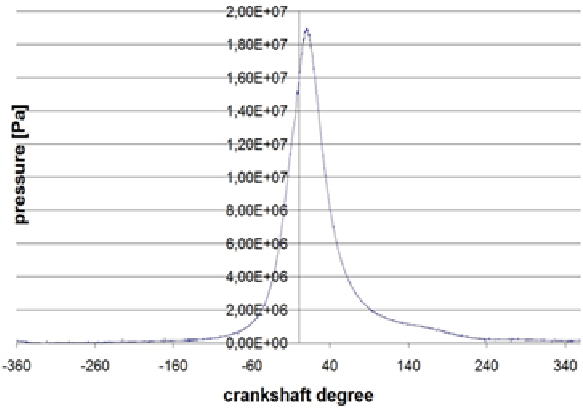

Figure-3. Indicator diagram.

1.2. Material properties and velocity of application of loads

Loads are applied on the piston at very high velocity and acceleration (see Figure-3 indicator diagram). In this condition, both Young's Modulus and ultimate tensile stress are sensibly higher than quasi-static values. In particular Yield stress tends to approach ultimate tensile stress and the material tends to lose its ductility. Stress to velocity data are very difficult to obtain.

Since pressure gradients are very steep, with values that may easily arrive up to 1.3×10^8 [bar/s], the increment of pressure inside the cylinder is extremely fast. The crystals that constitute the material do not have the time to modify their properties and the dynamic modulus of elasticity is incremented nearly up to the values of room temperature. For this particular alloy this relationship is kept up to 550°C. Practically, a hardening process takes places inside the material that deforms plastically, keeping the mechanical properties typical of much lower temperatures.

The law of plastic flux is the following (1):

$$\sigma = C\,(d\varepsilon/dt)^m \qquad (1)$$

where σ [psi] is the stress and ε is the deformation [-], while C and m are material constants. C and m for the Aluminum alloy 390.0-T5 are summarized in Table-3.

Table-3. Aluminum alloy 390.0 T5 a constants.

Temperature (˚C)	C (ksi)	**m** [-]
200	11,6	0,066
400	4,4	0,115
500	2,1	0,211

Table-3 shows that m increases four folds with the temperature that varies from 200 a 500 ˚C, so as temperature raised also the stress associated to the same strain rate increases four folds. So as temperature increase the influence of the deformation rate on maximum allowable stress increases. This means that the reaction

delay to the load (or inertia) of the material increases with the temperature. The higher the deformation rate the lower the stress felt by the material for instantaneous loads. This fact is more true as temperature raises. Table-4 gives the true elastic modulus with a pressure gradient of 1.3x108 [bar/s]. With this stress rate, the influence of temperature is limited to 70,000/48,000 =1.48 for the tangential Elastic Modulus and 135/65=2 for the Yield Stress. With static loads the elastic modulus reduction would have been the same (see Figure-1) while the Yield Stress reduction is more than 248/2=124 (see Figure-2). Practically the material doesn't resist to any static stress over 350°C. On the contrary, at high stress rate and for an extremely short time, the material is still resistant up to 500°C. This is due to the material inertia. This is the reason why models based on a liquid behavior instead of a solid one are used for explosive and bullet impact simulations.

Table-4. A390 T5 alloy material properties with a combustion chamber pressure gradient of $1.3x10^8$ [bar/s], the data were extrapolated from experimental data from forging of parts of the same material and simulations with and explicit FEA code.

Temperature [°C]	Modulus of Elasticity [MPa]	Yield stress [MPa]	Ultimate stress [MPa]
497	48,000	65	80
483	48,000	63	82
412	60,000	70	100
330	62,000	75	105
314	68,000	80	110
292	68,000	82	110
263	68,000	130	200
256	68,000	130	200
233	70,000	130	200
208	70,000	135	208

2. THE FEA WITH THE PROPOSED LINEARIZED MODEL

In our case the analysis starts from experimental data with lower-than-required thermal loads and power output (Figure-4). This makes it possible to tune the thermodynamic simulation model and to upgrade it to the required power level [5-12].

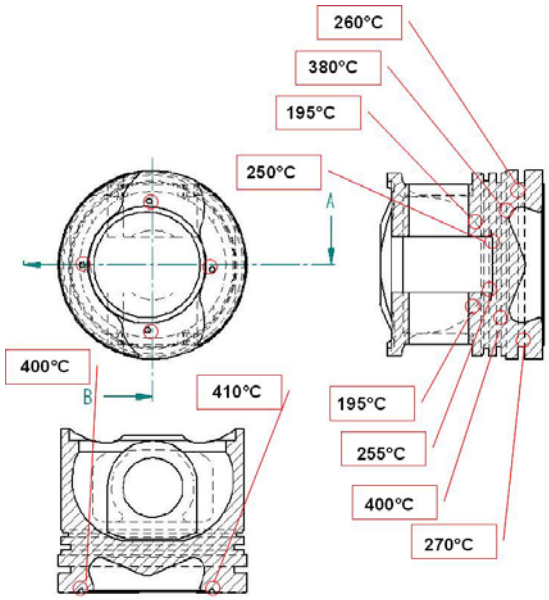

Figure-4. Shows the experimental temperature measured on piston with the original thermal load.

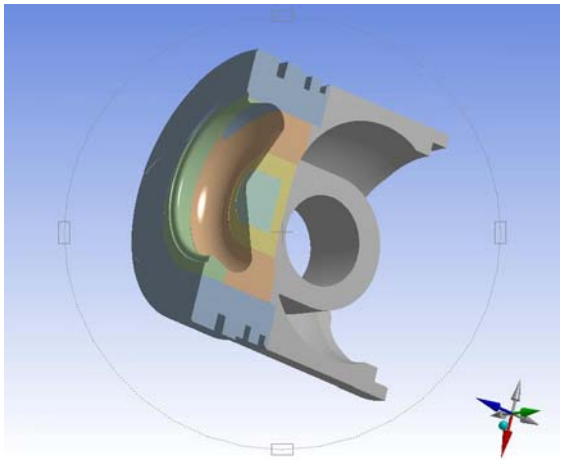

Figure-5. Different volumes with different peak temperatures (green=487°C, blue=483°C, brown=333°C, yellow=383°C, greyblue=412°C (center combustion chamber), blue=283°C, grey=213°C).

In Figure-5 the different volumes for the different temperature peak level are depicted. The software considers these zones as perfectly adherent, so congruence of displacements is automatically imposed on boundary surfaces.

3. COMPUTING

3.1. Linear FEA mesh [13-16]

Figure-6 shows the FEA mesh with the due refinement.

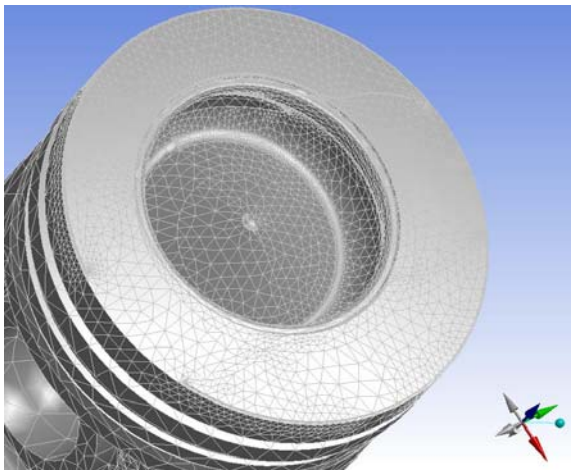

Figure-6. Mesh for linear solution.

The software takes the assembly as is and it "creates" a mesh. Due refinement is then added on fillet and geometrically complicated points.

3.2. Constraints

The piston should slide in the cylinder and for this purpose it has been considered the constraint through the rings. The piston can also freely rotate around the piston pin.
Figures 7 and 8 show the constraint on FE model.

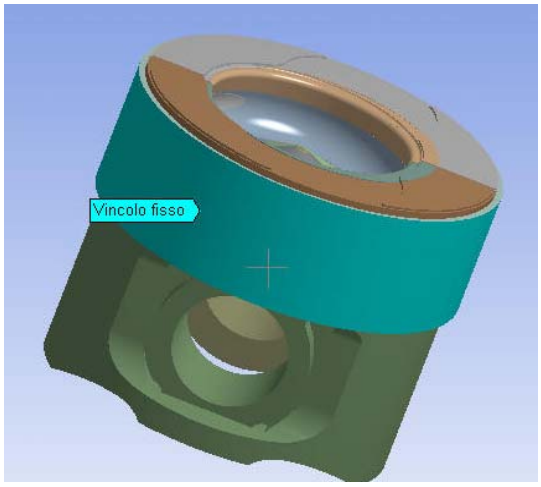

Figure-7. Ring constraint that simulates cylinder wall (green). "vincolo fisso" means "fixed constraint" and it is applied to the external surface of the ring.

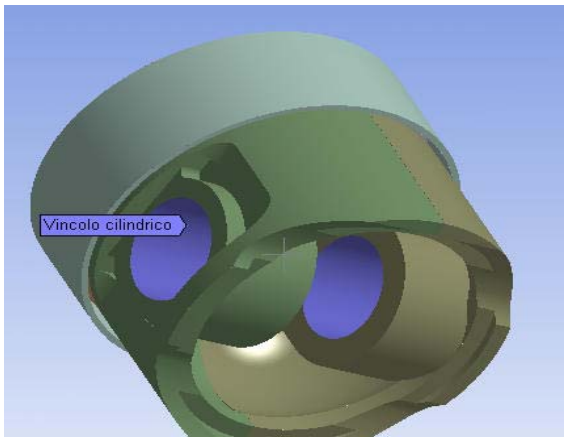

Figure-8. Cylindrical constraint that simulates the pin. "Vincolo cilindrico" means bearing constraint and it is applied to the two cylindrical surfaces (blue color) where the pins works.

3.3. Loads

The total load that affects the piston is composed by the pressure load and by the thermal load.

The thermal load is already embedded in the model through volumes with different material properties, so only the pressure loads should be applied.

The pressure load is simulated by the application of different pressure on different piston top surfaces. The different pressure values have been evaluated through the simplified method of Piancastelli [17-21]. Average values of 160 bar inside the combustion chamber and of 140 bar on the remaining piston surface have been applied on the FEA model both for the nonlinear and linear analysis.

3.4. Results of the simplified analysis

Figures 9 and 10 show stress fields and safety factors from FEA simulation. The piston was loaded with a pressure of 180 bar in the combustion chamber and of 160 bar on the piston top.

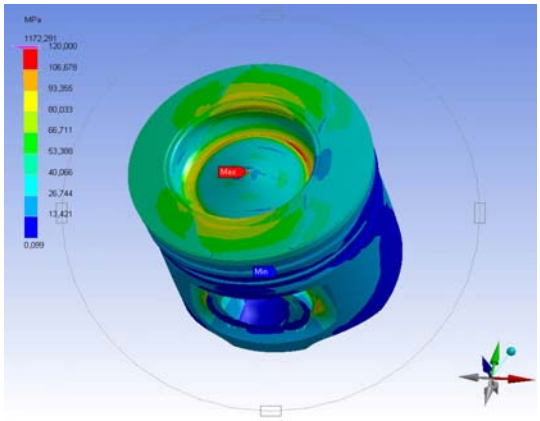

Figure-9. Pressure stresses at 160-180 bar from 120 MPa (red) down to 13.4 MPa (dark blue). The maximum value of 1172 MPa is not depicted in this Figure and depends on boundary condition on a coarsely modeled sharp edge.

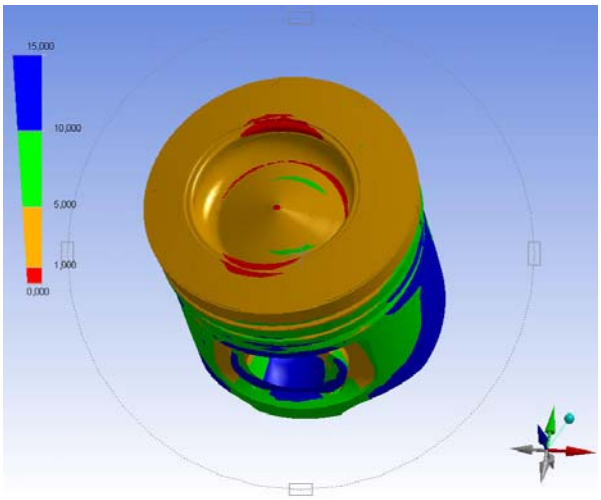

Figure-10. Safety factor at 160-180 bar from 15 (dark blue) down to values inferior to 1.00 (red). The original piston is not verified at this pressure level.

In Figure-10 it can be seen that the piston does not resist in the internal fillet of the combustion chamber. In fact the red color indicates that the material safety factor is less than 1. The safety factor is calculated as the ratio between the calculated stress and the yield stress. The only feasible solution is to change piston geometry, by increasing the fillet or by expanding the combustion chamber inside the piston. A flatter and less profound combustion chamber is a first solution; another possible solution is to improve piston cooling through a duct inside the piston. The larger fillet solution is adopted in Figure-11. This solution makes it possible to increase significantly the safety factor up to a minimum value of 2.

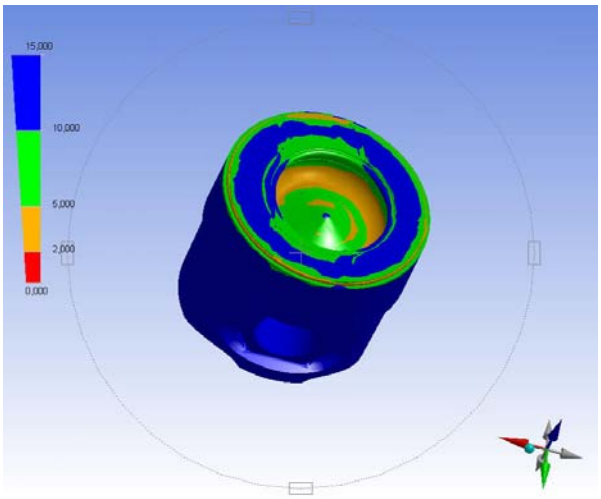

Figure-11. New geometry with pressure 140(outside the combustion chamber)-160 bar (inside the combustion chamber). No red color is present and the safety factor is everywhere above 2.

3.5. Nonlinear FEA mesh

A traditional nonlinear model has been implemented in order to compare the simplified linear approach with the traditional nonlinear solution. In order to make it possible to obtain a solution in a reasonable time only the half of the piston has been considered. For this purpose they have been used 10-nodes tetrahedral elements. The constraints and the loads are the same of the previous linearized model.
Figure-12 shows the nonlinear mesh.

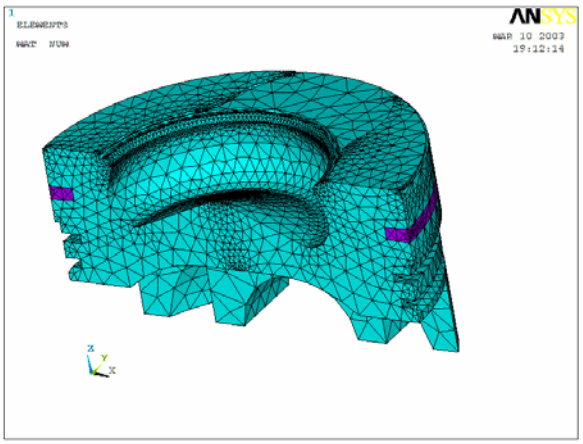

Figure-12. Nonlinear mesh.

3.6. Non liner analysis

The thermal flow value and the faces (walls) exchange coefficients have considered as following:

- Adiabatic faces(walls) of the piston;
- Thermal flow consequently found;
- Material characteristics, constraint system and thermal and structural loads as above.

Figures 13, 14 and 15 show the thermal and pressure loads and the boundary conditions.

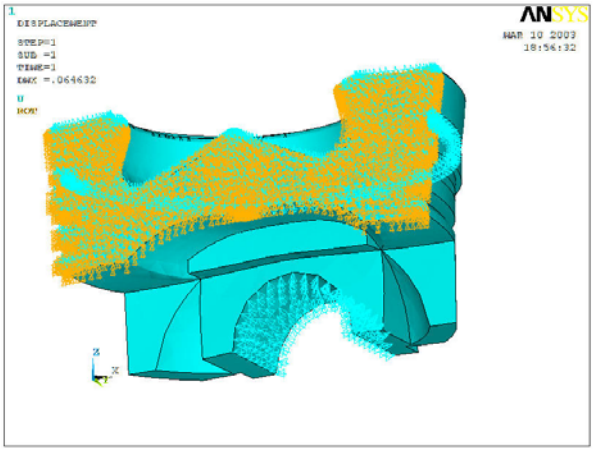

Figure-13. Constraints, only half of the piston was simulated. Even with this simplification, two whole days of computer time were necessary.

It has been necessary to impose the symmetrical constraint in order to analyze only an half of the piston (yellow arrows in Figure-13). Cylindrical constraints were also added in the piston-pin contact area. A radial boundary condition was added to simulate piston rings.

The temperature application field goes from a maximum of 490˚C on the top (red) to 208˚C (green) at the bottom of the piston, as it can be seen in Figure-14. No blue values are present on the piston in the results.

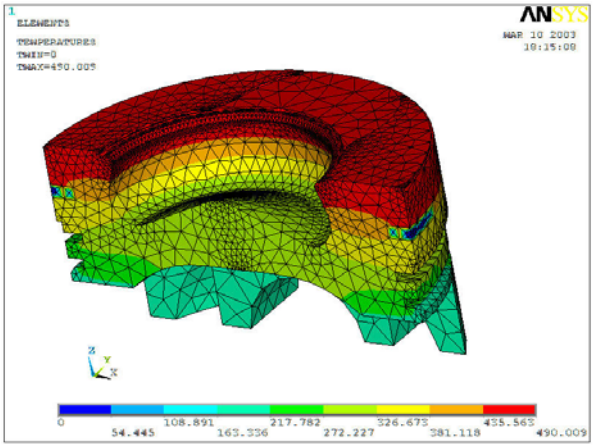

Figure-14. Temperature distribution.

The results depicted in Figure-15 show that the original piston cannot bear a maximum pressure of 160 bar, the combustion chamber fillet (red) is again the critical point [22-30]. This is the same result of the linearized model proposed. This calculation took 2 days of computer time on our best computer (a 256 Gygabite RAM PC), while the linearized simplified method proposed in this paper took less than 5 minute on a very common laptop.

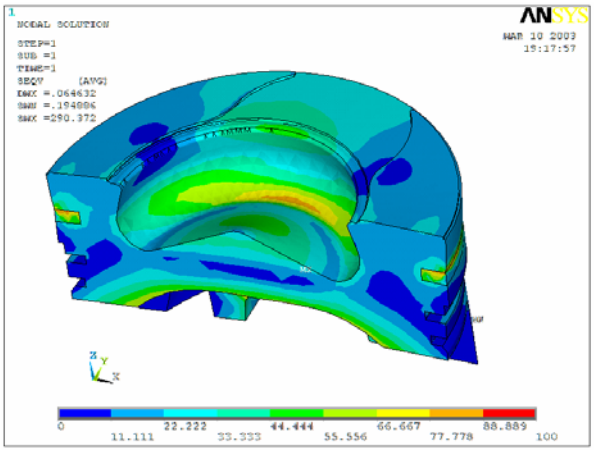

Figure-15. Nonlinear FEA results on the original piston with a peak pressure of 180 bar and a chamber pressure on piston top of 160 bar.

4. CONCLUSIONS

The linearized analysis gives the same results even on a very "difficult" component like an aluminium-alloy-diesel-direct-injection piston. This validates the method at least for aluminum alloy components, similar analysis have been performed on high temperatures alloys with even better accordance between linearized and nonlinear analysis. The components have then been tested on the engines with increased performance. No experimental data were collected on the upgraded parts with the new higher power level. However the new parts run without problems.

The linearized method, with its very reduced convergence time, makes it possible to optimize the components, operation that is not feasible with nonlinear analysis even with modern supercomputers. This is due to the fact that the linearized method always converge to a solution in a very limited computer time (<5min on a laptop), while the same piston with a standard nonlinear model took two days of computer time (>48h) on our very best PC. We considered us lucky that the model converged after this time. This fact is uncommon and manual steps should be usually performed to reach convergence. The results of the proposed linearized method and the nonlinear model are very similar. The maximum stress for the nonlinear analysis is 100 MPa (see Figure-15), while the linearized method gave 106 MPa (see Figure-9). The point of maximum stress is very close. The maximum value in the center of the combustion chamber of the linearized model (about 120 MPa) should not be considered since it is due to distorted FE elements (see Figure-9).

REFERENCES

[1] Kuchemann D. and Weber J. 1953. Aerodynamics of propulsion. Mc Graw-Hill.

[2] Kays W.M. and London A.L. 1955. Compact Heat Exchanger. Mc Graw-Hill.

[3] Hoerner S.F. 1965. Fluid Dynamic Drag. Hoerner.

[4] Gothert B. 1939. The Drag of Airplane Radiators with special References to Air Heating. NACA report n°896.

[5] Winter H. 1939. Contribution to the Theory of the Heated Duct Radiator. NACA report n°893.

[6] Meredith F.W. 1935. Note on the Cooling of Aircraft Engines with special references to Ethylene Glycol Radiators Enclosed in Ducts. British A.R.C. memorandum n°1683.

[7] Weise A. 1938. The Conversion of Energy in a Radiator. NACA report n°869.

[8] Nelson W.J., Czarnecki K.R. and Harrington R.D. 1944. Full-Scale Wind-Tunnel Investigation of Forward Underslung Cooling-Air Ducts. NACA report n°L115.

[9] Czarnecki K.R. and Nelson W.J. 1943. Wind-Tunnel Investigation of Rear Underslung Fuselage Ducts. NACA report n°L438.

[10] Ames Research Staff, Equations. 1953. Tables and Charts for Compressible Flow. NACA report n°1135.

[11] Johnston J Ford. 1943. Review of flight tests of NACA C and D cowlings on the XP-42 airplane. naca- report-771.

[12] C. McLemore. 1962. Wind Tunnel Tests of a 1/20-Scale Airship Model with Stern Propellers. NASA-TN-1026, Technical Note, Langley Research Center, January.

[13] AI AA-26-2693, "Aerodynamic design of Low Speed Aircraft with a NASA fuselage Wake/propeller Configuration", October 20-22 1986/Dayton Ohio

[14] Lowry and John T. 1999. The Bootstrap Approach to Aircraft Performance. Part Two, Constant-Speed Propeller Airplanes, December 12.

[15] Russian TsAGI. Spinning the fuselage to save fuel. www.flightglobal.com/.../russian-tsagi-spinning-the-fuselage-to-save-fuel.

[16] Piancastelli L. and Pellegrini M. 2007. The bonus of aircraft piston engines, and update on the Meredith effect. Int. Jour. Of Heat and Technology. 25(2): 51-56.

[17] Kurzke J. Achieving maximum thermal efficiency with the simple gas turbine cycle. MTU Aero Engines, Dachauer Str. 665, 80995 München, Germany.

[18] 2002. Gas Properties as a Limit to Gas Turbine Performance, R. C. Wilcock, J. B. Young and J. H. Horlock, ASME GT-2002-30517.

[19] L. Piancastelli, G. Caligiana, Frizziero Leonardo and S. Marcoppido. 2011. Piston engine cooling: an evergreen problem. 3rd CEAS Air and Space Conference - 21st AIDAA Congress - Venice (Italy), 24th-28th October.

[20] L. Piancastelli, L. Frizziero, E. Morganti and A. Canaparo. 2012. Fuzzy control system for aircraft diesel engines" edizioni ETS. International journal of heat and technology. ISSN 0392-8764. 30(1): 131-135.

[21] L. Piancastelli, L. Frizziero, S. Marcoppido and E. Pezzuti. 2012. Methodology to evaluate aircraft piston engine durability edizioni ETS. International journal of heat and technology. ISSN 0392-8764. 30(1): 89-92.

[22] L. Piancastelli, L. Frizziero, G. Zanuccoli, N.E. Daidzic and I. Rocchi. 2013. A comparison between CFRP and 2195-FSW for aircraft structural designs. International Journal of Heat and Technology. 31(1): 17-24.

[23] L. Piancastelli, L. Frizziero, N.E. Daidzic and I. Rocchi. 2013. Analysis of automotive diesel conversions with KERS for future aerospace applications. International Journal of Heat and Technology. 31(1): 143-154.

[24] L. Piancastelli, L. Frizziero and I. Rocchi. 2012. An innovative method to speed up the finite element analysis of critical engine components. International Journal of Heat and Technology. 30(2): 127-132.

[25] L. Piancastelli, L. Frizziero and I. Rocchi. 2012. Feasible optimum design of a turbocompound Diesel Brayton cycle for diesel-turbo-fan aircraft propulsion. International Journal of Heat and Technology. 30(2): 121-126.

[26] L. Piancastelli, L. Frizziero, S. Marcoppido, A. Donnarumma and E. Pezzuti. 2011. Fuzzy control system for recovering direction after spinning. International Journal of Heat and Technology. 29(2): 87-93.

[27] L. Piancastelli, L. Frizziero, S. Marcoppido, A. Donnarumma and E. Pezzuti. 2011. Active antiskid system for handling improvement in motorbikes controlled by fuzzy logic. International Journal of Heat and Technology. 29(2): 95-101.

[28] L. Piancastelli, L. Frizziero, E. Morganti and E. Pezzuti. 2012. Method for evaluating the durability of aircraft piston engines. Published by Walailak Journal of Science and Technology The Walailak Journal of Science and Technology, Institute of Research and Development, Walailak University, ISSN: 1686-3933, Thasala, Nakhon Si Thammarat 80161. 9(4): 425-431, Thailand.

[29] L. Piancastelli, L. Frizziero, E. Morganti and A. Canaparo. 2012. Embodiment of an innovative system design in a sportscar factory. Published by Pushpa Publishing House, "Far East Journal of Electronics and Communications. ISSN: 0973-7006. 9(2): 69-98, Allahabad, India.

[30] L. Piancastelli, L. Frizziero, E. Morganti and A. Canaparo. 2012. The Electronic Stability Program controlled by a Fuzzy Algorithm tuned for tyre burst

issues. Published by Pushpa Publishing House. Far East Journal of Electronics and Communications. ISSN: 0973-7006. 9(1): 49-68, Allahabad, India.

[31] L. Piancastelli, L. Frizziero, I. Rocchi, G. Zanuccoli and N.E. Daidzic. 2013. The "C-triplex" approach to design of CFRP transport-category airplane structures. International Journal of Heat and Technology, ISSN 0392-8764. 31(2): 51-59.

[32] L. Frizziero and I. Rocchi. 2013. New finite element analysis approach. Published by Pushpa Publishing House. Far East Journal of Electronics and Communications. ISSN: 0973-7006. 11(2): 85-100, Allahabad, India.

[33] L. Piancastelli, L. Frizziero and E. Pezzuti. 2014. Aircraft diesel engines controlled by fuzzy logic. Asian Research Publishing Network (ARPN). Journal of Engineering and Applied Sciences. ISSN 1819-6608. 9(1): 30-34, 2014, EBSCO Publishing, 10 Estes Street, P.O. Box 682, Ipswich, MA 01938, USA.

[34] L. Piancastelli, L. Frizziero and E. Pezzuti. 2014. Kers applications to aerospace diesel propulsion. Asian Research Publishing Network (ARPN). Journal of Engineering and Applied Sciences. ISSN 1819-6608. 9(5): 807-818, EBSCO Publishing, 10 Estes Street, P.O. Box 682, Ipswich, MA 01938, USA.